



**University of  
Zurich**<sup>UZH</sup>

**Zurich Open Repository and  
Archive**

University of Zurich  
Main Library  
Strickhofstrasse 39  
CH-8057 Zurich  
[www.zora.uzh.ch](http://www.zora.uzh.ch)

---

Year: 2016

---

## **Massively Parallelized Pollen Tube Guidance and Mechanical Measurements on a Lab-on-a-Chip Platform**

Shamsudhin, Naveen; Laebli, Nino; Atakan, Huseyin Baris; Vogler, Hannes; Hu, Chengzhi; Haeberle, Walter; Sebastian, Abu; Grossniklaus, Ueli; Nelson, Bradley J

DOI: <https://doi.org/10.1371/journal.pone.0168138>

Posted at the Zurich Open Repository and Archive, University of Zurich

ZORA URL: <https://doi.org/10.5167/uzh-130965>

Accepted Version



Originally published at:

Shamsudhin, Naveen; Laebli, Nino; Atakan, Huseyin Baris; Vogler, Hannes; Hu, Chengzhi; Haeberle, Walter; Sebastian, Abu; Grossniklaus, Ueli; Nelson, Bradley J (2016). Massively Parallelized Pollen Tube Guidance and Mechanical Measurements on a Lab-on-a-Chip Platform. PLoS ONE, 11(12):e0168138.

DOI: <https://doi.org/10.1371/journal.pone.0168138>



## 25 **Abstract**

26 Pollen tubes are used as a model in the study of plant morphogenesis, cellular  
27 differentiation, cell wall biochemistry, biomechanics, and intra- and intercellular  
28 signaling. For a “systems-understanding” of the bio-chemo-mechanics of tip-  
29 polarized growth in pollen tubes, the need for a versatile, experimental assay  
30 platform for quantitative data collection and analysis is critical. We introduce a  
31 Lab-on-a-Chip (LoC) concept for high-throughput pollen germination and pollen  
32 tube guidance for parallelized optical and mechanical measurements. The LoC  
33 localizes a large number of growing pollen tubes on a single plane of focus with  
34 unidirectional tip-growth, enabling high-resolution quantitative microscopy. This  
35 species-independent LoC platform can be integrated with micro-/nano-  
36 indentation systems, such as the cellular force microscope (CFM) or the atomic  
37 force microscope (AFM), allowing for rapid measurements of cell wall stiffness  
38 of growing tubes. As a demonstrative example, we show the growth and  
39 directional guidance of hundreds of lily (*Lilium longiflorum*) and Arabidopsis  
40 (*Arabidopsis thaliana*) pollen tubes on a single LoC microscopy slide.  
41 Combining the LoC with the CFM, we characterized the cell wall stiffness of lily  
42 pollen tubes. Using the stiffness statistics and finite-element-method (FEM)-  
43 based approaches, we computed an effective range of the linear elastic moduli  
44 of the cell wall spanning the variability space of physiological parameters  
45 including internal turgor, cell wall thickness, and tube diameter. We propose the  
46 LoC device as a versatile and high-throughput phenomics platform for plant  
47 reproductive and development biology using the pollen tube as a model.

48

49

## 50 **Introduction**

51 Pollen tubes are one of the fastest, if not the fastest, growing cellular systems  
52 with *in vivo* growth speeds reaching around 2.7  $\mu\text{m/s}$  in maize and only rivaled  
53 in the natural world by specially cultured neuronal cells [1]. The maize pollen  
54 starts to germinate within 5 minutes after contact with the stigma [2] and can  
55 grow 300 mm long in the style to fertilize the ovary, amassing along its journey

56 a record length-diameter ratio of around 12,000. This rapid tip-growth is driven  
57 by a dynamic and precisely regulated process involving ionic exchange, cell  
58 wall material metabolism, and cytoskeletal activity [3], necessitating high-  
59 throughput-assay platforms for phenotypic quantification.

60

61 Conventional *in vitro* assays for phenotyping pollen grains and pollen tubes use  
62 multi-well plates with liquid or agar-based gel media. The spatiotemporal growth  
63 of pollen tubes is highly disordered and three-dimensional in nature with  
64 crossovers and entanglement between tubes. Furthermore, the poor adhesion  
65 of grains and pollen tubes to the substrate makes long-term quantitative  
66 analysis via high-resolution microscopy and micro-indentation difficult. The need  
67 for computer-vision assisted automation to ‘track multiple, overlapping pollen  
68 tube trajectories in fluorescent time-lapse images’ was raised at the Third  
69 Annual Pollen RCN Meeting in 2013 [4]. Real-time automation methods for  
70 micro-indentation and optical monitoring have recently been introduced [5,6],  
71 but they require costly hardware accessories to existing microscopes.  
72 Conventional *in vitro* assays lack the precise spatiotemporal control of electro-  
73 chemical stimuli in the microenvironment of the growing cells needed to study  
74 cell-cell signaling and chemo-electro tropism and guidance mechanisms, which  
75 are key to successful *in vivo* fertilization.

76

77 Microfluidics and Lab-on-a-Chip (LoC) technologies are widely used in animal  
78 cell, tissue, and organ-level research [7–9]. The crossover of these technologies  
79 into plant sciences has been limited, but is growing. Phenotyping of entire *A.*  
80 *thaliana* plants and organs, such as roots and shoots, have been demonstrated  
81 through LoC platforms like the PlantChip [10] and RootArray [6]. Pioneering  
82 work at the cellular level was reported by Palanivelu, Zohar and colleagues  
83 [11,12], where a microfluidic chip was developed to simulate the anisotropic  
84 diffusion of ovule attractants towards *A. thaliana* pollen tubes. The TipChip and  
85 its variants have been used to study the influence of obstacles and chemical  
86 targeting on the growth of *Camellia japonica* pollen tubes as shown by  
87 Geitmann and colleagues [13,14]. Higashiyama and coworkers have used

88 *Torenia fournieri* to study pollen tube guidance and pollen tube-female tissue  
89 interaction and *A. thaliana* ovules for long-term live imaging [15,16] using  
90 specialized LoCs. All but one [15] of the above mentioned systems for pollen  
91 tubes studies lack the tight vertical confinement of the tip-growing cell in a  
92 single focal plane, which is crucial for long-term optical imaging and monitoring.  
93 The devices have a uniform height to accommodate the large size of the grain  
94 in comparison to the pollen tube, while Horade and colleagues cleverly avoided  
95 the need for a multi-height device by introducing a hand-pollinated style directly  
96 into the LoC [15]. The throughput of most existing LoC-based assays is  
97 restricted, however, as only a limited number of pollen tubes could be  
98 incorporated, guided, and observed on the chip at a time. There have been  
99 attempts at LoC-based systems for mechanical characterization of pollen tubes,  
100 but they also suffer from low-throughput [14,17] and their closed-cell  
101 architecture does not allow interfacing to calibrated micro-indentation [5], micro-  
102 gripping [18,19], micro-injection [20], or nano-indentation [21] systems for  
103 quantitative biomechanical characterization of the cell wall and cytoplasm.

104

105 Two of the most widely researched pollen tube model systems are *Lilium*  
106 *longiflorum* and *Arabidopsis thaliana*. Lily pollen tubes have historically been  
107 the model of choice, ever since the first electron microscopy studies of its  
108 ultrastructure [22]. Since then several physiological processes and parameters  
109 have been studied and quantified with this model, such as internal turgor  
110 pressure [23], pH and  $\text{Ca}^{2+}$  concentrations [24]. The relatively large geometric  
111 size, high *in vitro* germination rate and growth speed, and robustness of the  
112 pollen and pollen tube have been reasons for its choice as a model. With the  
113 recent release of a high quality lily pollen transcriptome [25], we believe that the  
114 use of *L. longiflorum* as a model will increase, requiring high-throughput  
115 analysis platforms. *A. thaliana* on the other hand offers the advantages of a  
116 short generation cycle, small size, and a well understood genome,  
117 transcriptome, and proteome [26–30]. With powerful forward and reverse  
118 genetic approaches, a wide mutant catalog exists for genotype-phenotype  
119 mapping. Till recently, large-scale phenotypic *in vitro* analysis of *Arabidopsis*

120 pollen tubes was hindered by low pollen germination and growth rates [31,32],  
121 most likely due to lack of growth-promoting molecules found in the female pistil.  
122 Nevertheless, Arabidopsis pollen remains the most studied model for pollen  
123 tube growth and its regulation.

124

125 In this paper, we report the concept of a species-independent LoC platform for  
126 long-term, high-resolution optical observation and mechanical measurements of  
127 pollen tubes. We show devices specifically tailored to study *L. longiflorum* and  
128 *A. thaliana* pollen tubes. We have demonstrated the unidirectional growth of  
129 hundreds of lily and Arabidopsis pollen tubes with no significant changes in  
130 growth parameters such as morphology, germination, and growth rates as  
131 compared to conventional *in vitro* plate culture. We demonstrate the integration  
132 of the LoC device with the CFM [5,33,34] to characterize the cell wall stiffness  
133 of lily pollen tubes. The high-throughput mechanical measurements of the LoC-  
134 CFM combination in conjunction with FEM modeling allowed us to determine  
135 the uncertainty estimates of the linear elastic moduli of the lily pollen tube cell  
136 wall. We believe that this LoC platform will significantly aid bio-chemo-  
137 mechanical phenotyping as well as systems-modeling of the mechanisms  
138 governing pollen tube growth.

139

## 140 **Materials and methods**

### 141 **Lab-on-a-Chip device fabrication**

142 The photolithography mask is designed using Siemens NX CAD software and  
143 printed in film by Selba A.G, Switzerland. From the photomask to the final LoC  
144 device, the process entails a two-step photolithography followed by PDMS  
145 casting, cutting, and glass bonding (see Fig A in S1 Appendix). In the first step,  
146 commercial photo-curable polymer SU8 (Microchem Corp, U.S.A) is spin-cast  
147 onto a 4 inch silicon wafer to reach the desired micro-channel height. After soft-  
148 baking on a hot-plate, the wafer is exposed to UV light with the first layer mask  
149 to generate the channels. After a post-exposure baking, the unpolymerized  
150 resist is washed off and baking is done once again to make the mold

151 mechanically stable and adherent to the silicon substrate. A second layer of  
152 SU8 is spun-cast to the height required for the grain chamber, and the baking,  
153 exposure, resist removal, and baking steps are repeated to generate the two-  
154 height SU8 mold. Then PDMS is poured into the mold under a vacuum pump  
155 and baked at 80 °C to crosslink the PDMS. After cooling, the PDMS can be  
156 peeled off and then cut into the required size. A 1.5 mm biopsy punch needle is  
157 used to punch the fluid inlet holes and the PDMS chip is cleaned with tape. An  
158 oxygen plasma chamber is then used to bond the PDMS to a microscopy slide  
159 or coverslip. To improve adhesion of the pollen tubes to the device after they  
160 grow out of the microchannels of the LoC, the glass slide is coated with poly-L-  
161 lysine.

162

## 163 **Plant material**

164 Lily (*Lilium longiflorum*) flowers are purchased from the local florist in Zurich and  
165 the anthers excised and individually placed in Eppendorf tubes and kept at -  
166 80 °C for storage. On the day of experimentation, the Eppendorf tube with the  
167 anther is allowed to equilibrate to room temperature for 30 minutes at 100 %  
168 humidity. The culture medium for pollen germination consists of: 160 µM H<sub>3</sub>BO<sub>3</sub>,  
169 130 µM Ca(NO<sub>3</sub>)<sub>2</sub>, 1 mM KNO<sub>3</sub>, 5 mM MES, 10 % sucrose at a pH of 5.6. For  
170 conventional *in vitro* studies, the pollen is brushed onto microscopy slides and  
171 then covered with a few drops of growth medium. For in-chip studies, the  
172 culture medium is added into the anther-containing Eppendorf tube, and the  
173 system is allowed to imbibe for thirty minutes before the mixture of culture  
174 media and pollen grains are taken up into a syringe for loading into the LoC  
175 device.

176

177 *Arabidopsis* [*Arabidopsis thaliana* (L.) Heynh., accession Columbia (Col-0)]  
178 plants are grown under controlled long-day conditions at 22 °C and 60 %  
179 relative humidity. Dehiscent flowers are harvested and kept at 100 % relative  
180 humidity for pollen rehydration for about 30 minutes. To collect the pollen  
181 grains, approximately 30 flowers are immersed in a 2 ml Eppendorf tube  
182 containing 1.5 ml of pollen germination medium (1.6 mM H<sub>3</sub>BO<sub>3</sub>, 5 mM CaCl<sub>2</sub>, 5

183 mM KCl, 1 mM MgSO<sub>4</sub>, 10% sucrose, pH 7.5). Flowers are slightly squeezed  
184 with tweezers, then briefly vortexed. After centrifugation at 950 rcf for 2 minutes,  
185 floral tissue is removed with tweezers. The pollen grains are pre-incubated at  
186 22 °C in the Eppendorf tube for 30-60 minutes before loading into the LoC  
187 device.

188

## 189 **Germination and growth in LoC device**

190 After pre-incubation in the growth medium the grains are injected into the LoC  
191 inlet with light pressure using a microsyringe. The loading pressure flushes the  
192 grains from the inlet into the grain reservoir, while the liquid medium flushes in  
193 through the microchannels, which are open at the end. Each unit cell is  
194 individually filled with the grain/growth medium mixture. A droplet of growth  
195 medium is placed on top of each inlet, and the LoC is placed in a humid  
196 environment and under controlled temperature. The first pollen tubes germinate  
197 and enter the channel within an hour of incubation.

198

## 199 **Micro-Indentation with the Cellular Force Microscope**

200 The hardware of the micro-indentation system is identical to that described by  
201 Felekis and colleagues [5]. The targeted growing pollen tube is located with the  
202 inverted microscope. The sensor tip is positioned as close as possible to the  
203 pollen tube. First, a coarse approach is performed with the coarse positioners to  
204 find the location of the glass surface. This approach step is controlled to  
205 approximately 500-600 nm/sec and, after the contact to the glass slide the  
206 sensor tip is lifted up by 70 μm. The tip is then positioned over the tube and a  
207 fine approach and micro-indentation is performed using piezo-positioners. A  
208 maximal loading force of 5 μN and a loading/unloading speed of 2 μm/sec is  
209 used across the experiments. The measurements are done with the LoC, the  
210 sensor tip and the pollen tube completely immersed in the growth medium.  
211 There is no active fluid flow and the large fluidic volume around the LoC  
212 ensures that there is minimal evaporation during the course of measurements.  
213 The capillary stiffness experienced by the sensor tip is two orders of magnitude



214 lower than the stiffness of the tube cell wall and is thus neglected. The force-  
215 indentation data is processed in MATLAB and the sensor stiffness is cancelled  
216 from each dataset to yield the true force-indentation curve (see Fig B in S1  
217 Appendix). An image is captured with the inverted microscope immediately after  
218 every indentation to determine the position of the indenter with respect to the  
219 growing tube. The apparent stiffness defined as the slope in the region of  
220 maximum load is calculated for the loading and unloading curve separately to  
221 account for the viscoelastic behavior of the pollen tube cell wall. For the FEM  
222 modeling, we only used the loading curve dataset.

223

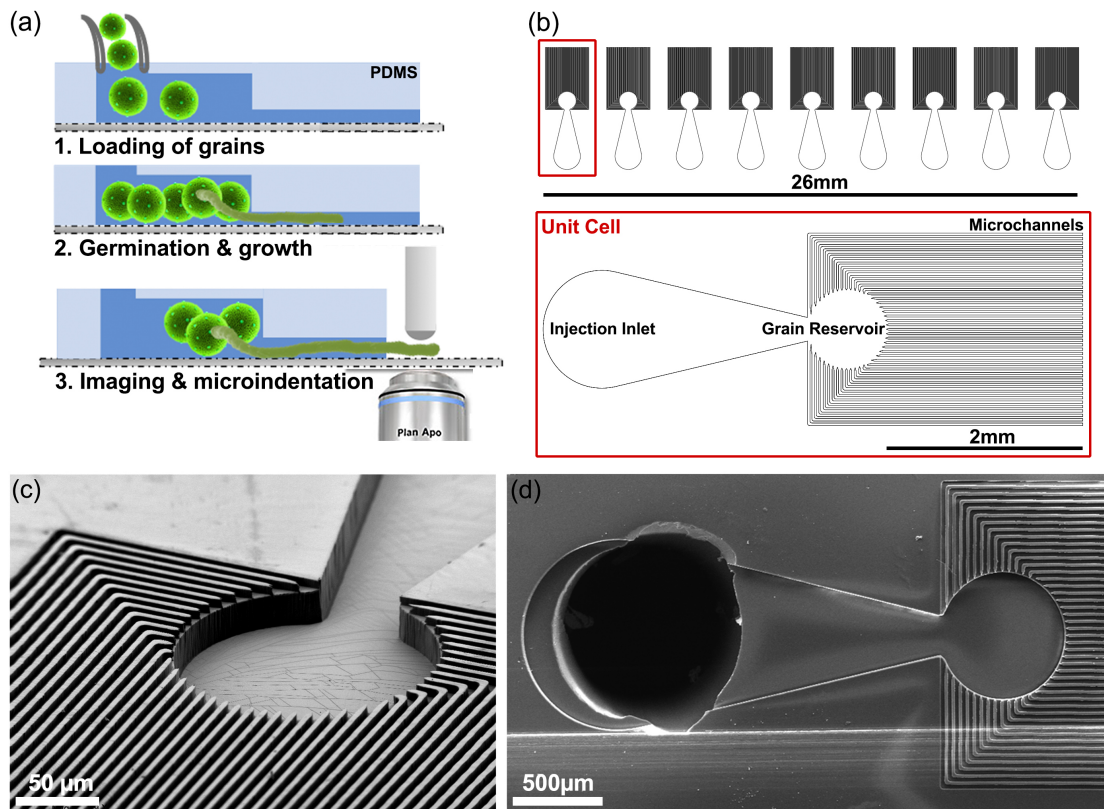
224

## 225 **Results and discussion**

### 226 **Design and fabrication of the Lab-on-a-Chip device**

227 The LoC design, demonstrated here for *L. longiflorum* (Fig 1), is a species-  
228 independent platform allowing for optical observation via bright field, differential  
229 interference contrast (DIC), or fluorescent-confocal microscopy of massively  
230 parallelized unidirectional growth of pollen tubes in the same focal plane. The  
231 vertical confinement of the tubes eliminates the need for constant objective  
232 refocusing for long-term microscopy and the single directional and parallelized  
233 guidance allows for easier automation and post-processing of growth rates and  
234 other morphological assessment. Furthermore, the open channel architecture of  
235 the chip (Fig 1a) enables interfacing with well-established experimental  
236 platforms, such as the CFM and AFM for mechanical and surface morphology  
237 characterization of the cell wall [35,36], or to micro-injection systems for intra-  
238 cellular injection of dyes or internal turgor pressure measurement [23], as well  
239 as for chemical, electrical, thermal, or osmotic modification of the micro- or  
240 macro-environment around the growing pollen tube [37–40]. The design easily  
241 allows for fluorescent dye loading via passive diffusion after germination [41]  
242 and by pressure shock in non-germinated pollen [42].

243



244

245 **Fig 1. Lab-on-a-chip (LoC) device**

246 (a) Design concept and functionality - The LoC is loaded with grains and  
 247 nutrient medium, the grains germinate, and the pollen tubes are self-guided into  
 248 the microchannels, allowing for massively parallelized optical imaging and  
 249 micro-indentation.

250 (b) The design layout of the lily LoC with a magnified view of an individual cell.

251 (c),(d) Scanning electron micrographs of the fabricated PDMS chip for lily.

252

253 The basic functional unit of the LoC, called the unit cell (Fig 1b), consists of  
 254 three sections: (i) a large circular fluidic chamber that serves as the inlet for  
 255 loading a pollen-growth medium, (ii) a grain reservoir connected to the inlet via  
 256 a tapering neck, and (iii) dozens of collinear microchannels emerging from the  
 257 grain reservoir. Guided by the injection fluid pressure, the grains flow through  
 258 the inlet into the grain reservoir where they can germinate. The surrounding  
 259 channels guide the pollen tubes during growth and parallelize their growth in a  
 260 unidirectional trajectory in the same focal plane. Our two-height microfluidic chip

261 is fabricated via two-step photo-lithography, followed by soft-replica molding of  
262 polydimethylsiloxane (PDMS), which allows for a higher height for the pollen  
263 grain chambers with the tubes growing in a narrower channel (Fig 1c). The  
264 choice of PDMS for the device is due to its optical transparency, low  
265 autofluorescence, high permeability to oxygen and carbon dioxide, low cost,  
266 and ease of device fabrication.

267

268 Each lily LoC occupies a 26x10 mm space with nine identical unit cells placed  
269 next to each other (Fig 1b). In comparison, a standard microscopy slide has  
270 dimensions of 75x26 mm. Each unit cell has 44 microchannels emerging from  
271 the grain chamber allowing for a theoretical maximum of  $9 \times 44 = 396$  tubes to be  
272 simultaneously and unidirectionally guided. Considering that the lily pollen tube  
273 must grow up to 120 mm through the style to fertilize the female gametophyte,  
274 and pollen growth rates of 100-500 nm/sec have been recorded, we designed  
275 the chip such that the shortest microchannel is 2 mm in length and the longest  
276 3.4 mm, which allows for the observation of several hours of growth.

277

278 From a design and fabrication point of view, there is no technical limitation on  
279 the maximum channel length that can be made by this process. Shorter channel  
280 lengths allow for reduced experimental time in micro-indentation studies, as the  
281 pollen tubes grow out of the microchannels onto the glass slide quicker. This  
282 can be easily achieved by shortening the PDMS channel length by a blade-cut.  
283 With the non-uniform length distribution of the channels, the traversal length for  
284 each potentially guided pollen tube is different, allowing for sequential micro-  
285 indentation as they emerge out of the channels. To tailor the exact dimensions  
286 for the lily and Arabidopsis chip variants, we assumed the geometry of the  
287 pollen grains to be well approximated by a prolate ellipsoid and the pollen tube  
288 by a right-circular cylinder. We measured a major diameter of  $128.5 \pm 9.9 \mu\text{m}$   
289 and minor diameter of  $98.3 \pm 5.8 \mu\text{m}$  for lily pollen ( $n=40$ ) and, correspondingly,  
290  $27.0 \pm 1.8 \mu\text{m}$  and  $19.9 \pm 1.1 \mu\text{m}$  for Arabidopsis pollen ( $n=40$ ). The tube  
291 diameters are  $17.4 \pm 2.5 \mu\text{m}$  and  $4.9 \pm 0.7 \mu\text{m}$  for lily and Arabidopsis ( $n=40$ ),  
292 respectively. For the lily LoC, the design width and height of the channels are

293 chosen to be 25  $\mu\text{m}$  and 30  $\mu\text{m}$ , respectively, allowing for adequate flow of  
294 nutrients and non-constricted growth of the pollen tube in the channel. We  
295 achieved a width of  $24.9\pm 0.7$   $\mu\text{m}$  and height of  $31.9\pm 0.7$   $\mu\text{m}$  as confirmed by the  
296 analysis of SEM images (Fig 1c,1d). The depth of the inlet region and the grain  
297 reservoir is  $118.5\pm 9$   $\mu\text{m}$  (design value of 120  $\mu\text{m}$ ), allowing the flow of grains  
298 without multilayering or stacking.

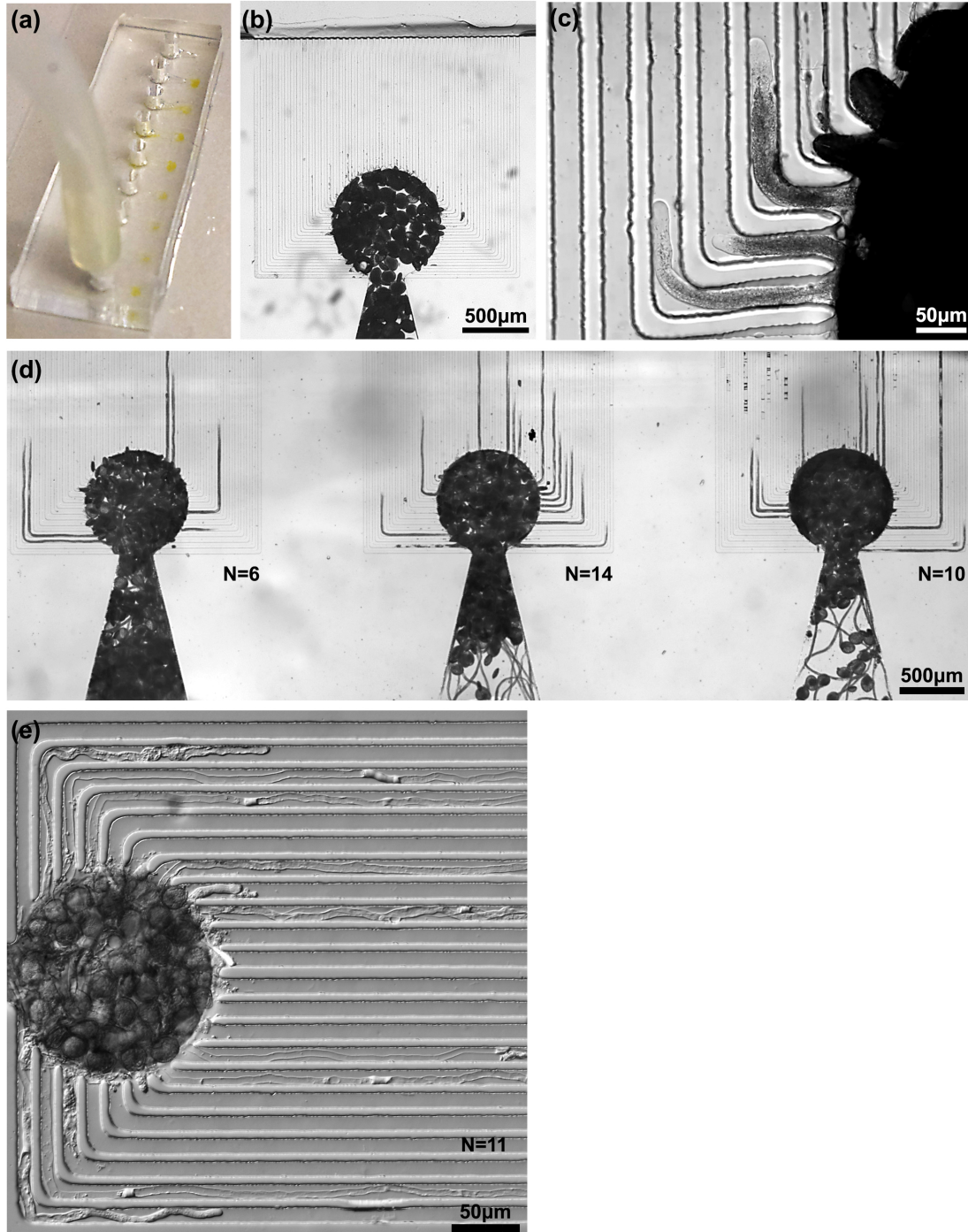
299

### 300 **Germination, growth and parallel guidance**

301 The germination rate of lily grains seems to be unaffected in the LoC and the  
302 tube morphology looked similar to those of control tubes grown on liquid  
303 medium-based slide assays. We recorded an average of 12 pollen tubes guided  
304 per unit cell (n=34) 7 hours after chip-loading (Fig 2a,2b,2c,2d), yielding an  
305 equi-focal unidirectional guidance of  $9\times 12=108$  lily tubes per LoC device. Such  
306 high rates of parallelized, directional tube growth without entanglement, allows  
307 quantitative phenotyping at unprecedented rates. Moreover, there is no change  
308 in diameter of the pollen tubes in the chip ( $17.31\pm 2.4$   $\mu\text{m}$ , n=18) compared to  
309 control tube diameters. The lily tubes showed regular oscillatory tip growth [43]  
310 (see Fig C in S1 Appendix) and the average *in chip* growth rate is 189 nm/sec  
311 (n=14) compared to an *in vitro* control rate of 272 nm/sec (n=14). The viability of  
312 the tubes is not affected as *in vitro* growth rates with a high variability of 100-  
313 500 nm/sec have been reported in the literature [39,44]. *Torenia fournieri* pollen  
314 tubes grown in microchannels have been reported to show a 2.5 times  
315 enhanced growth rate compared to normal liquid medium assay (n=16), and it  
316 was speculated that the microchannels mimic an *in vivo* growth environment for  
317 the pollen tubes [15]. In the TipChip [13], it was observed that changing the  
318 microchannel-height to tube-diameter ratio from 4.7 to 9.4 increased the growth  
319 rate by up to 50% (n=3) for *Camellia japonica*, but no control data on  
320 conventional *in vitro* growth rates was presented. We also achieved a large  
321 guidance rate for *Arabidopsis* pollen tubes in the LoC device (Fig 2e). The  
322 average number of tubes guided per unit cell was 6 (n=24 cells). The  
323 *Arabidopsis* LoC design dimension accommodates 40 unit cells because of the  
324 smaller grain and tube size as compared to lily. With the increase in unit cells

325 per LoC, we can thus uni-directionally guide on average  $6 \times 40 = 240$  Arabidopsis  
326 tubes per chip.

327



328

329 **Fig 2. Germination, growth, and parallel guidance of pollen tubes in the**  
330 **LoC device.**

331 (a) The LoC is injected with nutrient medium containing lily pollen grains that  
332 become concentrated and appear as yellowish circles.

333 (b) A view of a lily unit cell immediately after injection of grains.

334 (c) Three lily pollen tubes are guided into neighboring channels and can be  
335 simultaneously imaged at high magnification.

336 (d) A stitch of the three unit cells shows the equifocal unidirectional guidance of  
337 a large number of lily pollen tubes

338 (e) This stitch shows the guidance of eleven *A. thaliana* pollen tubes in a single  
339 unit cell.

340 N = number of tubes guided in a unit cell.

341

342 No tube growth inhibition due to the L-shaped bends of the channel is  
343 observed. The tubes successfully navigated the bends without a change in  
344 growth rate. Even in sharp bends no tip bursting is observed (Fig 2c) and the  
345 pollen tubes are able to grow through the entire length of the channels and exit  
346 the PDMS device onto the glass slide. After exiting the channels, the tubes  
347 grow in a straight direction for several hundred micrometers before changing to  
348 a random growth direction. This single-directional growth is important for robust  
349 localization and automation of single cell mechanical indentation studies. The  
350 growth in the microchannels is reminiscent of *in vivo* conditions in the stylar  
351 matrix, which force individual pollen tubes to navigate maze-like trajectories to  
352 reach the female gametophyte. After germination, lily pollen tubes traverse  
353 through a hollow pistilar environment, adhering to the epidermal cells aligning  
354 the transmitting channel while, in *Arabidopsis*, the pollen tubes penetrate the  
355 cell wall of stigmatic papillar cells and grow intercellularly through the  
356 transmitting tissue to reach the ovules [45].

357

358 To demonstrate the low auto-fluorescence and compatibility of the LoC device  
359 with fluorescence microscopy, we labeled the cell wall using propidium iodide  
360 (PI) and monitored intracellular calcium concentration using the dye Calcium  
361 Green<sup>TM</sup>-1 AM (see Fig D in S1 Appendix). While lily pollen tubes can be loaded  
362 with fluorescent dyes via particle bombardment, electroporation, or - less

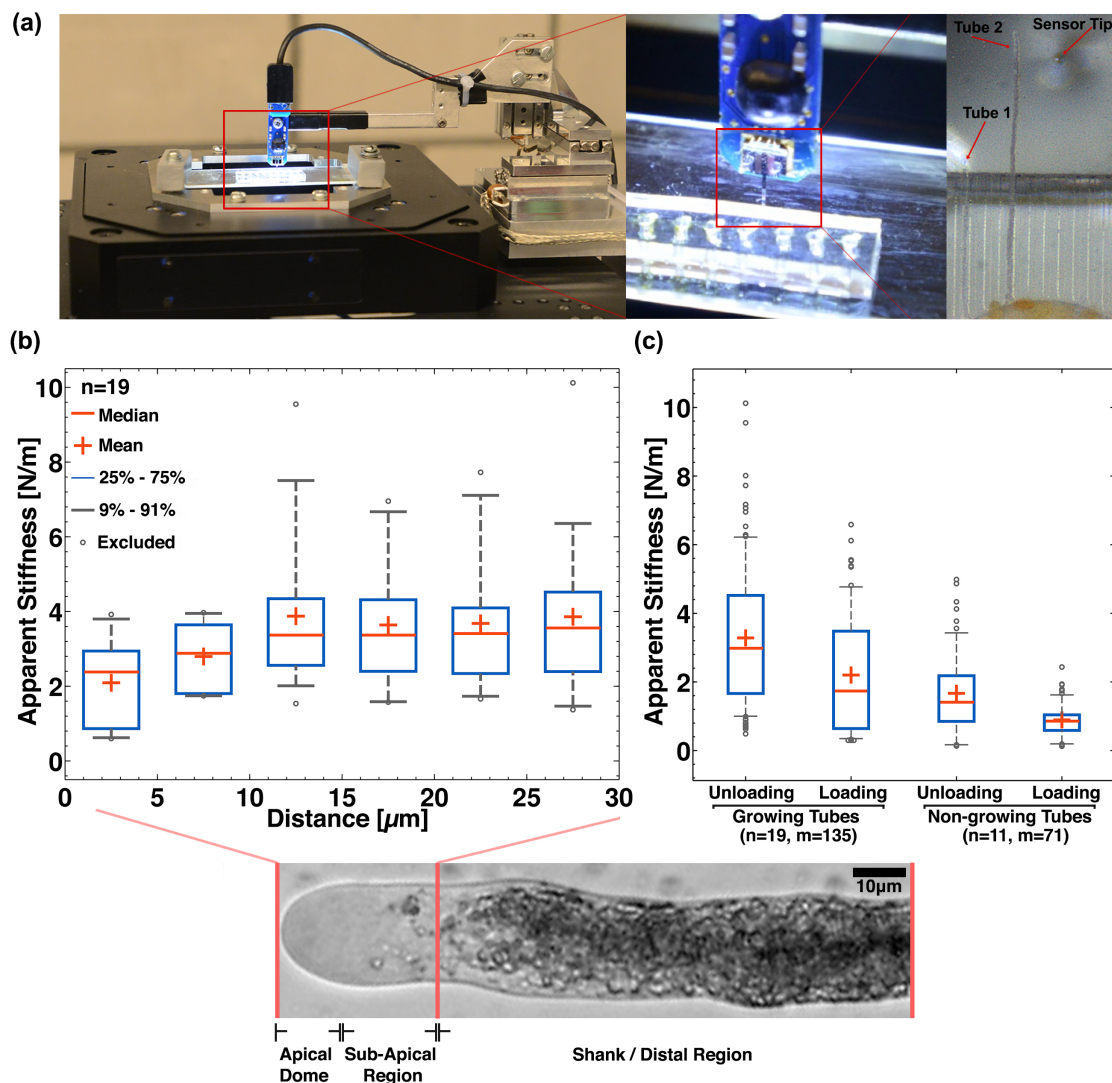
363 invasively - by osmotic pressure [42], we chose to use the cell wall permeable  
364 AM-ester form of Calcium Green (albeit its low sub-cellular resolution and  
365 sequestering into vesicles) and PI because it can be co-incubated with the  
366 tubes in the growth medium.

367

## 368 **Integration with Cellular Force Microscope for high-** 369 **throughput micro-indentation**

370 The cell wall is a heterogeneous structural network of polysaccharides and  
371 proteins, and the understanding of its bio-chemo-mechanics is of utmost  
372 scientific, agricultural, and socioeconomic interest, arising from the use of plant  
373 cell wall material for food, feed, fiber, fuel, paper, wood, adhesives, coatings,  
374 and thickeners [46]. The regulation of the spatiotemporal rheology of the cell  
375 wall is crucial for cellular differentiation and morphogenesis, as well as for  
376 mechanical stability and restraint against pathogens and environmental factors  
377 like wind, rain, and composition of the ground. Complementary to organism and  
378 tissue level studies on mechanical aspects of growth and morphogenesis,  
379 pollen tubes are an ideal *in vitro* system for studying biomechanics at a cellular  
380 level. Previously reported micro-indentation studies on pollen tubes suffered  
381 from low measurement throughput and have mostly used micron-sized indenter  
382 geometries - *Papaver rhoeas* (pollen tube diameter,  $d_t < 10 \mu\text{m}$  and indenter tip  
383 diameter,  $\Phi = 3\text{-}4 \mu\text{m}$  [47]), *Solanum chacoense* ( $d_t < 10 \mu\text{m}$   $\Phi = 10 \mu\text{m}$  [48]),  
384 *A. thaliana* ( $d_t \sim 5 \mu\text{m}$   $\Phi = 3\text{-}4 \mu\text{m}$  [49]) and *L. longiflorum* ( $14 < d_t < 20 \mu\text{m}$   $\Phi =$   
385  $4 \mu\text{m}$  [50] and  $\Phi = 0.8 \mu\text{m}$  [51]). A high-throughput micro-mechanical  
386 characterization system is achieved by integrating the LoC device with the well-  
387 established CFM platform (Fig 3a). After germination and guidance, when the  
388 first tubes begin to emerge from the microchannels, rapid micro-indentation is  
389 performed on the tubes within the first  $200 \mu\text{m}$  of their growth outside the  
390 channel with a sub-micron tipped-indenter (tip diameter,  $\Phi = 800 \text{nm}$ , see Fig E  
391 in S1 Appendix). The microchannel guidance enables a predictable and uni-  
392 directional growth of the tubes out of the PDMS chip onto the poly-L-lysine  
393 coated glass slide (Fig 3a). This ensures increased cellular localization and

394 adhesion for performing rapid micro-indentation. The slope of the measured  
 395 force-indentation curve is defined here as the *apparent stiffness*, since the  
 396 curve does not solely represent the mechanical behavior of the cell wall, but  
 397 also the contribution of the cell and indenter geometry, along with the cell's  
 398 turgor pressure. In general, the curves exhibit mild hysteresis or viscoelastic  
 399 behavior (see Fig B in S1 Appendix) and, hence, we calculated the loading and  
 400 unloading apparent stiffness separately.  
 401



402  
 403 **Fig 3. System integration of the LoC with the Cellular Force Microscope**  
 404 **and micro-indentation dataset.**

405 (a) High-throughput micro-indentation measurements are possible because  
 406 directionally guided tubes emerge out of the channels.



407 (b) The apparent stiffness (unloading) of growing tubes is measured along the  
408 length of the tube near the apex region.

409 (c) The apparent stiffness (loading and unloading) of the shank area of growing  
410 lily tubes compared to that of non-growing tubes. ( $n$  denotes the number of  
411 tubes and  $m$  denotes the total number of indentations on  $n$  tubes)

412

413

414 We perform micro-indentation along the length of growing lily pollen tubes  
415 ( $n=19$ ). The force-indentation curves reveal a reduction in the measured  
416 apparent stiffness at the apex of the pollen tube compared to the distal region  
417 as shown in Fig 3b. We believe that the measurement of reduced apical  
418 stiffness is the result of at least two effects, the change in contact-geometry  
419 between probe and pollen tube cell wall and also the gradient in the  
420 biochemical constituency of the cell wall along the length of the pollen tube  
421 [51,52]. The contact-angle of micro-indentation at the apical dome is less than  
422  $90^\circ$ , leading to a reduction in the reaction force acting along the force-sensor  
423 axis. Secondly, cell wall staining shows a gradient in molecular composition  
424 across the length of the lily pollen tube [53]. The apical dome is rich in methyl-  
425 esterified pectins and non-crystalline cellulose compared to the distal region.  
426 De-esterified pectins are absent in the apical dome and are found uniformly  
427 across the shank area. Lastly, the presence of callose steadily increases from  
428 the apex to the distal region and crystalline cellulose is present in uniform  
429 intensity across the whole length of the tube. A combination of the gelatinous  
430 nature of the methyl-esterified pectin concentrated at the apex and the  
431 geometric effect of a non-normal contact indentation can lead to the reduced  
432 stiffness measurements at the apex. With conventional single-axis micro-  
433 indentation methods, it is difficult to differentiate between these two effects, and  
434 multi-degree of freedom force sensors [54,55] or AFM-based nano-indentation  
435 techniques are needed to determine the contribution of the geometry and  
436 biochemical composition effects.

437

438 We compared the apparent stiffness of the distal or shank region (50  $\mu\text{m}$  away  
439 from the tip) of growing lily pollen tubes to that of non-growing pollen tubes.  
440 Untriggered or natural growth-arrest, a state of negligible tube growth but  
441 displaying active internal streaming, is commonly observed in *in vitro* assays.  
442 The distal stiffness measured on growing pollen tubes (n=19, 135 indentations)  
443 can be characterized by the mean and median loading (unloading) stiffness of  
444 2.20 N/m (3.28 N/m) and 1.73 N/m (2.98 N/m), respectively (Fig 3c). The broad  
445 stiffness distribution is attributed to intra-cellular, inter-pollen, inter-anther, and  
446 inter-flower variability as the micro-indentation technique, in itself, is robust and  
447 repeatable. Compared to growing tubes, indentation of non-growing pollen  
448 tubes (n=11, 71 indentations) reveal a significant reduction in the mean loading  
449 (unloading) stiffness 0.69 N/m (1.67 N/m).

450

451 Naturally growth-arrested *Papaver rhoeas* tubes were previously reported to  
452 exhibit lower distal stiffness compared to growing tubes and this was posited to  
453 be due to reduced turgor pressure [56]. While it is well known from osmotic  
454 assays that a minimum level of turgor is necessary for pollen tube growth, no  
455 correlation was observed between internal turgor levels, measured and  
456 manipulated with a micropipette, and the growth rate in lily tubes [23]. While  
457 there has been no other direct measurements of turgor pressure in pollen  
458 tubes, micropipette-based techniques used on geometrically isotropic *Chara*  
459 *corallina* (green algae) cells have reported a linear correlation between growth  
460 and internal turgor [57]. The extension response of tip-growing fungal hyphae to  
461 changes in internal turgor show a more complicated relationship [58], with even  
462 reports of normal tip-growth in *S. ferax* taking place in the absence of any  
463 measurable turgor pressure, achieved through softening of the cell wall in the  
464 region of growth [59]. While an internal state of reduced turgor is a possibility,  
465 further micro-mechanical investigations using advanced tools like the fluidic  
466 AFM [60] could provide a means of simultaneous turgor manipulation and force-  
467 indentation on pollen tubes.

468

469 A comparative study of the mechanical properties of the cell wall across pollen  
470 species and measurement techniques based on apparent stiffness data is  
471 difficult because the measurements are specific to the particular indenter  
472 geometry used, the tube diameter, internal turgor pressure, cell wall thickness,  
473 and the biochemistry-induced mechanical anisotropy of its cell wall. Assuming a  
474 linear elastic material behavior of the cell wall combined with knowledge about  
475 cell wall thickness and internal turgor, one can estimate the effective Young's  
476 modulus for the entire cell wall using FEM-based modeling, taking into account  
477 the known geometrical parameters of the micro-indentation. The FEM-based  
478 modeling framework presented by Vogler and colleagues [51] is implemented  
479 and the effect of the biologically relevant variability in turgor, cell wall thickness,  
480 cell diameter, and the Young's modulus on the apparent stiffness during micro-  
481 indenter loading is investigated. We observe that several different combinations  
482 of these input parameters, and especially an order of magnitude spread in  
483 Young's moduli from 20 MPa to 400 MPa, yield similar values of loading  
484 stiffness (see Table A and Fig F in S1 Appendix). This is in the range of recently  
485 published measures of elastic moduli of plant cell walls, 20 and 90 MPa for lily  
486 pollen tubes [51], 280-420 MPa for *Camellia japonica* pollen tubes [17], and 50-  
487 757 MPa for *Nicotiana tabacum* Bright Yellow-2 (BY-2) cells [61]. Whole cell  
488 compression tests have been used to estimate the cell wall moduli of  
489 *Saccharomyces cerevisiae* to be between 107-112 MPa, which are fairly  
490 consistent within the various phases of growth [62]. The cell wall stiffness of  
491 fungal hyphae was quantified to be between 64-110 MPa using quasi-static  
492 AFM [63].

493

494 These micro-indentation studies show that we need a statistical approach to  
495 quantify the mechanics of the pollen tube cell wall. One should refrain from  
496 using a single value attribution to either the apparent stiffness or the effective  
497 linear elastic moduli of the pollen tube cell wall. A key reason is that the cell wall  
498 is a heterogenous polymer with spatiotemporal modulation of its underlying  
499 biochemistry. It is also due to the currently unobservable dynamic nature of cell  
500 wall thickness and turgor pressure, which vary depending on the growth

501 environment *in vivo* or *in vitro*. Importantly we must note that the estimate of the  
502 Young's modulus is highly dependent on the underlying modeling approach  
503 used, and this explains the discrepancies between the estimates in literature,  
504 which have utilized different modeling approaches. Quantified measurements of  
505 turgor pressure, effective cellular stiffness and a consistent modeling paradigm  
506 to determine the cell wall elastic moduli need to be established, if we are to  
507 unravel the mechanisms underlying pollen tube growth and penetration through  
508 the stylar matrix.

509

## 510 **Conclusions**

511 We designed and introduced a LoC device for germination, growth, and  
512 unidirectional guidance of hundreds of pollen tubes in the same focal plane.  
513 The two chip designs demonstrated in this paper for lily and Arabidopsis can be  
514 directly used for other well-studied pollen tube models. The lily chip with its 25  
515  $\mu\text{m}$  wide channels can be used to guide *Camellia japonica* (camellia), *Nicotiana*  
516 *tabacum* (tobacco), and *Zea mays* (maize) pollen tubes, while the Arabidopsis  
517 design can be used for *Papaver rhoeas* (poppy) and *Solanum chacoense* (wild  
518 potato) pollen tubes and fungal hyphae. Early adoption of these cost-effective  
519 LoC devices by the community can aid development of optimized in-chip  
520 germination and growth protocols for different wild type species and their  
521 mutant lines. The LoC devices are fully compatible with calibrated and robust  
522 micro-mechanical characterization platforms like the CFM, which ensure  
523 repeatability across studies on growth biomechanics. We used this integrated  
524 LoC-CFM platform for biomechanical characterization of growing and non-  
525 growing lily pollen tubes. Using the micro-indentation dataset, the uncertainty  
526 estimates in the physiological growth parameters and FEM modeling, we have  
527 shown that there exists a large range in the effective linear elastic moduli of the  
528 lily pollen tube cell wall. We believe that our LoC can serve the need for high-  
529 throughput, long-term live cell imaging and micro-mechanical characterization  
530 towards unraveling the causality chain between the oscillatory growth variables  
531 of ion fluxes, localized exocytosis, cell wall remodeling, turgor pressure, and

532 growth rates generating the fast tip-polarized cell growth in pollen tubes and  
533 fungal hyphae.

534

## 535 **Acknowledgements**

536 We thank Gautam Muglani, Mahmut Selman Sakar, Jan Burri (ETH Zürich),  
537 Christoph Ringli, Christoph Eichenberger, and Tohnyui Ndinyanka Fabrice  
538 (University of Zürich) for constructive discussions.

## References

1. Bedinger P. The remarkable biology of pollen. *Plant Cell*. 1992;4: 879–887. doi:10.1105/tpc.4.8.879
2. Dresselhaus T, Lausser A, Marton ML. Using maize as a model to study pollen tube growth and guidance, cross-incompatibility and sperm delivery in grasses. *Ann Bot*. 2011;108: 727–737. doi:10.1093/aob/mcr017
3. Feijó JA, Costa SS, Prado AM, Becker JD, Certal AC. Signalling by tips. *Curr Opin Plant Biol*. 2004;7: 589–598. doi:10.1016/j.pbi.2004.07.014
4. Cheung AY, Palanivelu R, Tang WH, Xue HW, Yang WC. Pollen and plant reproduction biology: Blooming from east to west. *Mol Plant*. The Authors. All rights reserved.; 2013;6: 995–997. doi:10.1093/mp/sst108
5. Felekis D, Vogler H, Mecja G, Muntwyler S, Nestorova A, Huang T, et al. Real-time automated characterization of 3D morphology and mechanics of developing plant cells. *Int J Rob Res*. 2015;/: 1–11. doi:10.1177/0278364914564231
6. Busch W, Moore BT, Martsberger B, Mace DL, Twigg RW, Jung J, et al. A microfluidic device and computational platform for high-throughput live imaging of gene expression. *Nat Methods*. 2012;9: 1101–1106. doi:10.1038/nmeth.2185
7. Takayama S, Ostuni E, LeDuc P, Naruse K, Ingber DE, Whitesides GM. Subcellular positioning of small molecules. *Nature*. 2001;411: 1016. doi:10.1038/35082637
8. Lucchetta EM, Lee JH, Fu LA, Patel NH, Ismagilov RF. Dynamics of *Drosophila* embryonic patterning network perturbed in space and time using microfluidics. *Nature*. 2005;434: 1134–1138. doi:10.1038/nature03461.1.
9. Esch EW, Bahinski A, Huh D. Organs-on-chips at the frontiers of drug discovery. *Nat Rev Drug Discov*. Nature Publishing Group; 2015;14: 248–260. doi:10.1038/nrd4539
10. Jiang H, Xu Z, Aluru MR, Dong L. Plant chip for high-throughput phenotyping of *Arabidopsis*. *Lab Chip*. 2014;14: 1281–93. doi:10.1039/c3lc51326b

11. Cooper JR, Qin Y, Jiang L, Palanivelu R, Zohar Y. Microsystem-based study of pollen-tube attractants secreted by ovules. Proceedings of the IEEE International Conference on Micro Electro Mechanical Systems (MEMS). IEEE; 2009. pp. 208–211.  
doi:10.1109/MEMSYS.2009.4805355
12. Yetisen AK, Jiang L, Cooper JR, Qin Y, Palanivelu R, Zohar Y. A microsystem-based assay for studying pollen tube guidance in plant reproduction. J Micromechanics Microengineering. 2011;21: 54018. doi:10.1088/0960-1317/21/5/054018
13. Agudelo CG, Nezhad AS, Ghanbari M, Naghavi M, Packirisamy M, Geitmann A. TipChip: A modular, MEMS-based platform for experimentation and phenotyping of tip-growing cells. Plant J. 2013;73: 1057–1068. doi:10.1111/tpj.12093
14. Sanati Nezhad A, Naghavi M, Packirisamy M, Bhat R, Geitmann A. Quantification of cellular penetrative forces using lab-on-a-chip technology and finite element modeling. Proc Natl Acad Sci U S A. 2013;110: 8093–8098. doi:10.1073/pnas.1221677110
15. Horade M, Yanagisawa N, Mizuta Y, Higashiyama T, Arata H. Growth assay of individual pollen tubes arrayed by microchannel device. Microelectron Eng. Elsevier B.V.; 2014;118: 25–28. doi:10.1016/j.mee.2014.01.017
16. Arata H, Higashiyama T. Poly(dimethylsiloxane)-based microdevices for studying plant reproduction. Biochem Soc Trans. 2014;42: 320–4. doi:10.1042/BST20130258
17. Nezhad AS, Naghavi M, Packirisamy M, Bhat R, Geitmann A. Quantification of the Young's modulus of the primary plant cell wall using Bending-Lab-On-Chip (BLOC). Lab Chip. 2013;13: 2599–608. doi:10.1039/c3lc00012e
18. Beyeler F, Neild A, Oberti S, Bell DJ, Sun Y, Dual J, et al. Monolithically fabricated microgripper with integrated force sensor for manipulating microobjects and biological cells aligned in an ultrasonic field. J Microelectromechanical Syst. 2007;16: 7–15.  
doi:10.1109/JMEMS.2006.885853
19. Bhargav SDB, Jorapur N, Ananthasuresh GK. Micro-scale composite compliant mechanisms for evaluating the bulk stiffness of MCF-7 cells. Mech Mach Theory.

- Elsevier Ltd; 2015;91: 258–268. doi:10.1016/j.mechmachtheory.2015.04.002
20. Sun Y, Nelson BJ. Biological cell injection using an autonomous microrobotic system. *Int J Rob Res*. 2002;21: 861–868. doi:10.1177/0278364902021010833
  21. Raman A, Trigueros S, Cartagena A, Stevenson a. PZ, Susilo M, Nauman E, et al. Mapping nanomechanical properties of live cells using multi-harmonic atomic force microscopy. *Nat Nanotechnol*. Nature Publishing Group; 2011;6: 809–814. doi:10.1038/nnano.2011.186
  22. Rosen WG, Gawlik SR, Dashek W V, Siegesmund KA. Fine structure and cytochemistry of *Lilium* pollen tubes. *Am J Bot*. 1964;51: 61–71.
  23. Benkert R, Obermeyer G, Bentrup F-W. The turgor pressure of growing lily pollen tubes. *Protoplasma*. 1997;198: 1–8. doi:10.1007/BF01282125
  24. Wilsen KL, Hepler PK. Sperm Delivery in Flowering Plants: The Control of Pollen Tube Growth. *Bioscience*. 2007;57: 835. doi:10.1641/B571006
  25. Lang V, Usadel B, Obermeyer G. De novo sequencing and analysis of the lily pollen transcriptome: an open access data source for an orphan plant species. *Plant Mol Biol*. 2015;87: 69–80. doi:10.1007/s11103-014-0261-2
  26. Arabidopsis Genome Initiative. Analysis of the genome sequence of the flowering plant *Arabidopsis thaliana*. *Nature*. 2000;408: 796–815. doi:10.1038/35048692
  27. Honys D, Twell D. Transcriptome analysis of haploid male gametophyte development in *Arabidopsis*. *Genome Biol*. 2004;5: R85.1-R.85.13. doi:10.1186/gb-2004-5-11-r85
  28. Pina C. Gene Family Analysis of the Arabidopsis Pollen Transcriptome Reveals Biological Implications for Cell Growth, Division Control, and Gene Expression Regulation. *Plant Physiol*. 2005;138: 744–756. doi:10.1104/pp.104.057935
  29. Loraine AE, McCormick S, Estrada A, Patel K, Qin P. RNA-Seq of Arabidopsis Pollen Uncovers Novel Transcription and Alternative Splicing. *Plant Physiol*. 2013;162: 1092–1109. doi:10.1104/pp.112.211441
  30. Grobei MA, Qeli E, Brunner E, Rehrauer H, Zhang R, Roschitzki B, et al. Deterministic



- protein inference for shotgun proteomics data provides new insights into Arabidopsis pollen development and function. *Genome Res.* 2009;19: 1786–1800.  
doi:10.1101/gr.089060.108
31. Boavida LC, McCormick S. Temperature as a determinant factor for increased and reproducible in vitro pollen germination in *Arabidopsis thaliana*. *Plant J.* 2007;52: 570–582. doi:10.1111/j.1365-313X.2007.03248.x
  32. Vogler F, Schmalzl C, Enghart M, Bircheneder M, Sprunck S. Brassinosteroids promote *Arabidopsis* pollen germination and growth. *Plant Reprod.* 2014;27: 153–167.  
doi:10.1007/s00497-014-0247-x
  33. Felekis D, Muntwyler S, Vogler H, Beyeler F, Grossniklaus U, Nelson BJ. Quantifying growth mechanics of living, growing plant cells in situ using microrobotics. *Micro Nano Lett.* 2011;6: 311. doi:10.1049/mnl.2011.0024
  34. Routier-Kierzkowska A-L, Weber a., Kochova P, Felekis D, Nelson BJ, Kuhlemeier C, et al. Cellular Force Microscopy for in Vivo Measurements of Plant Tissue Mechanics. *Plant Physiol.* 2012;158: 1514–1522. doi:10.1104/pp.111.191460
  35. Zhang T, Zheng Y, Cosgrove DJ. Spatial organization of cellulose microfibrils and matrix polysaccharides in primary plant cell walls as imaged by multichannel atomic force microscopy. *Plant J.* 2016;85: 179–192. doi:10.1111/tpj.13102
  36. Yakubov GE, Bonilla MR, Chen H, Doblin MS, Bacic A, Gidley MJ, et al. Mapping nano-scale mechanical heterogeneity of primary plant cell walls. *J Exp Bot.* 2016;67: 2799–2816. doi:10.1093/jxb/erw117
  37. Prado AM, Porterfield DM, Feijó JA. Nitric oxide is involved in growth regulation and re-orientation of pollen tubes. *Development.* 2004;131: 2707–2714. doi:10.1242/dev.01153
  38. Malhó R, Camacho L, Moutinho A. Signalling Pathways in Pollen Tube Growth and Reorientation. *Ann Bot.* 2000;85: 59–68. doi:10.1006/anbo.1999.0991
  39. Parton RM, Fischer-Parton S, Trewavas AJ, Watahiki MK. Pollen tubes exhibit regular periodic membrane trafficking events in the absence of apical extension. *J Cell Sci.*

- 2003;116: 2707–2719. doi:10.1242/jcs.00468
40. Haduch-Sendecka A, Pietruszka M, Zajdel P. Power spectrum, growth velocities and cross-correlations of longitudinal and transverse oscillations of individual *Nicotiana tabacum* pollen tube. *Planta*. 2014;240: 263–276. doi:10.1007/s00425-014-2083-5
  41. Altartouri B, Geitmann A. Understanding plant cell morphogenesis requires real-time monitoring of cell wall polymers. *Curr Opin Plant Biol*. Elsevier Ltd; 2014;23: 76–82. doi:10.1016/j.pbi.2014.11.007
  42. Rato C, Monteiro D, Hepler PK, Malhó R. Calmodulin activity and cAMP signalling modulate growth and apical secretion in pollen tubes. *Plant J*. 2004;38: 887–897. doi:10.1111/j.1365-313X.2004.02091.x
  43. Rounds CM, Hepler PK, Fuller SJ, Winship LJ. Oscillatory Growth in Lily Pollen Tubes Does Not Require Aerobic Energy Metabolism. *Plant Physiol*. 2010;152: 736–746. doi:10.1104/pp.109.150896
  44. Hepler PK, Lovy-Wheeler A, Mckenna ST, Kunkel JG. Ions and Pollen Tube Growth. In: Malhó R, editor. *The Pollen Tube*. Berlin/Heidelberg: Springer-Verlag; 2006. pp. 47–70. doi:10.1007/7089\_043
  45. Lord E. Adhesion and cell movement during pollination: Cherchez la femme. *Trends Plant Sci*. 2000;5: 368–373. doi:10.1016/S1360-1385(00)01744-1
  46. Cosgrove DJ. Creeping walls, softening fruit, and penetrating pollen tubes: the growing roles of expansins. *Proc Natl Acad Sci U S A*. 1997;94: 5504–5505. doi:10.1073/pnas.94.11.5504
  47. Geitmann A, Parre E. The local cytomechanical properties of growing pollen tubes correspond to the axial distribution of structural cellular elements. *Sex Plant Reprod*. 2004;17: 9–16. doi:10.1007/s00497-004-0210-3
  48. Parre E, Geitmann A. Pectin and the role of the physical properties of the cell wall in pollen tube growth of *Solanum chacoense*. *Planta*. 2005;220: 582–592. doi:10.1007/s00425-004-1368-5

49. Chebli Y, Kaneda M, Zerzour R, Geitmann A. The cell wall of the Arabidopsis pollen tube--spatial distribution, recycling, and network formation of polysaccharides. *Plant Physiol.* 2012;160: 1940–55. doi:10.1104/pp.112.199729
50. Zerzour R, Kroeger J, Geitmann A. Polar growth in pollen tubes is associated with spatially confined dynamic changes in cell mechanical properties. *Dev Biol.* Elsevier Inc.; 2009;334: 437–446. doi:10.1016/j.ydbio.2009.07.044
51. Vogler H, Draeger C, Weber A, Felekis D, Eichenberger C, Routier-Kierzkowska AL, et al. The pollen tube: A soft shell with a hard core. *Plant J.* 2013;73: 617–627. doi:10.1111/tpj.12061
52. Routier-Kierzkowska AL, Smith RS. Measuring the mechanics of morphogenesis. *Curr Opin Plant Biol.* Elsevier Ltd; 2013;16: 25–32. doi:10.1016/j.pbi.2012.11.002
53. Fayant P, Girlanda O, Chebli Y, Aubin C-E, Villemure I, Geitmann A. Finite element model of polar growth in pollen tubes. *Plant Cell.* 2010;22: 2579–2593. doi:10.1105/tpc.110.075754
54. Beyeler F, Muntwyler S, Nelson BJ. A six-axis MEMS force-torque sensor with micro-Newton and nano-Newtonmeter resolution. *J Microelectromechanical Syst.* 2009;18: 433–441. doi:10.1109/JMEMS.2009.2013387
55. Burri JT, Hu C, Shamsudhin N, Wang X, Vogler H, Grossniklaus U, et al. Dual-Axis Cellular Force Microscope for Mechanical Characterization of Living Plant Cells. (in Preparation). 2016.
56. Geitmann A, McConnaughey W, Lang-Pauluzzi I, Franklin-Tong VE, Emons AMC. Cytomechanical properties of papaver pollen tubes are altered after self-incompatibility challenge. *Biophys J.* 2004;86: 3314–23. doi:10.1016/S0006-3495(04)74379-9
57. Boyer JS. Cell wall biosynthesis and the molecular mechanism of plant enlargement. *Funct Plant Biol.* 2009;36: 383–394. doi:10.1071/FP09048
58. Lew RR. How does a hypha grow? The biophysics of pressurized growth in fungi. *Nat Rev Microbiol.* Nature Publishing Group; 2011;9: 509–518. doi:10.1038/nrmicro2591

59. Money NP, Harold FM. Two water molds can grow without measurable turgor pressure. *Planta*. 1993;190: 426–430. doi:10.1007/BF00196972
60. Gabi M, Behr P, Studer P, Niedermann P, Bitterli J, Liley M, et al. FluidFM: Combining Atomic Force Microscopy and Nanofluidics in a Universal Liquid Delivery System for Single Cell Applications and Beyond. *Nano Lett*. 2009;9: 2501–7.
61. Weber A, Braybrook S, Huflejt M, Mosca G, Routier-Kierzkowska AL, Smith RS. Measuring the mechanical properties of plant cells by combining micro-indentation with osmotic treatments. *J Exp Bot*. 2015;66: 3229–3241. doi:10.1093/jxb/erv135
62. Smith AE, Zhang Z, Thomas CR, Moxham KE, Middelberg P. The mechanical properties of *Saccharomyces cerevisiae*. *Proc Natl Acad Sci U S A*. 2000;97: 9871–4. doi:10.1073/pnas.97.18.9871
63. Zhao L, Schaefer D, Xu H, Modi SJ, LaCourse WR, Marten MR. Elastic properties of the cell wall of *Aspergillus nidulans* studied with atomic force microscopy. *Biotechnol Prog*. 2005;21: 292–299. doi:10.1021/bp0497233

## Supporting Information

**S1 Appendix. Contains supporting figures and the parametric finite element (FE) model and associated results.**

## S1 Appendix: Supporting Information

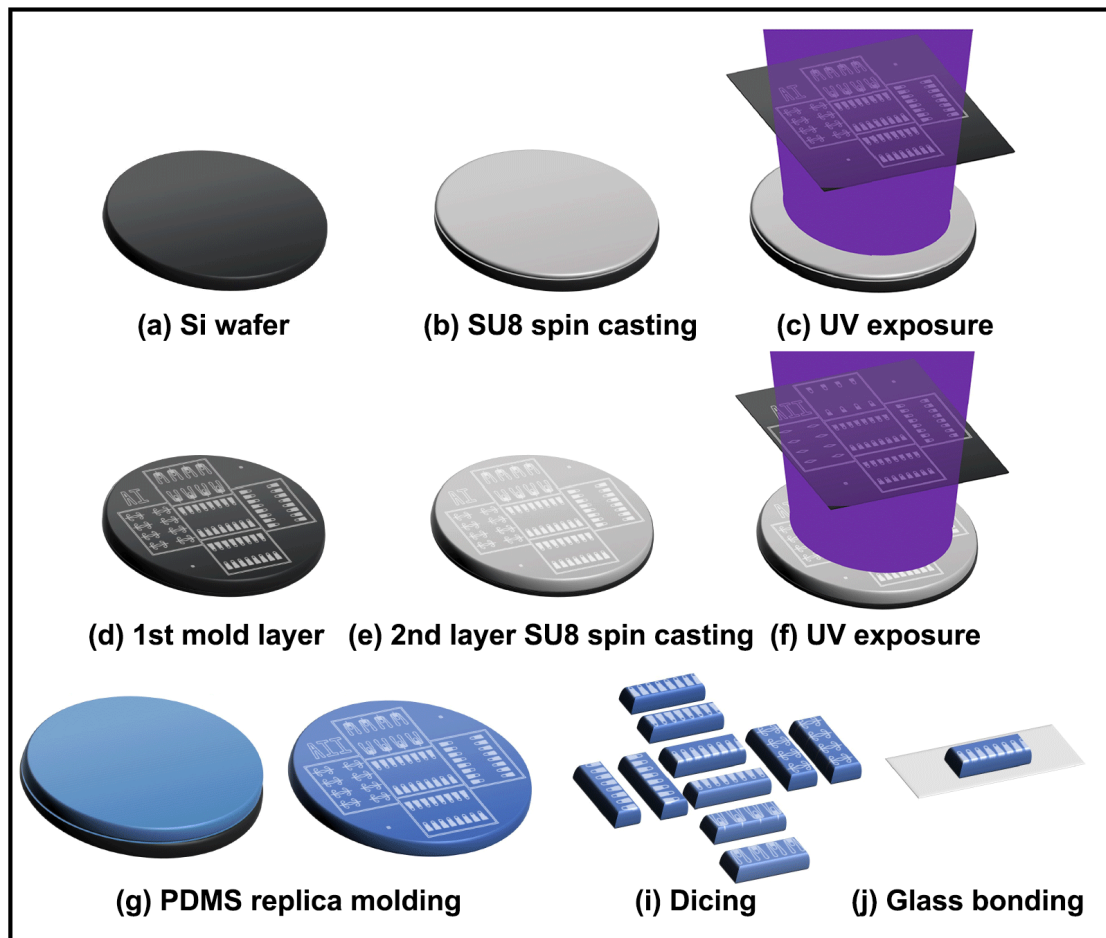


Fig A. Fabrication process of the Lab-on-a-Chip device.

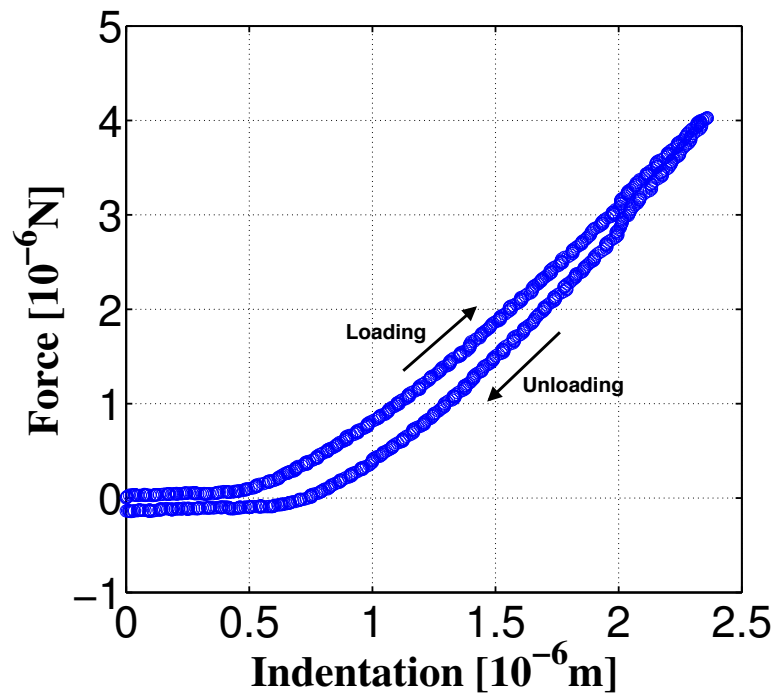


Fig B. An example of a force-indentation curve on lily pollen tube.

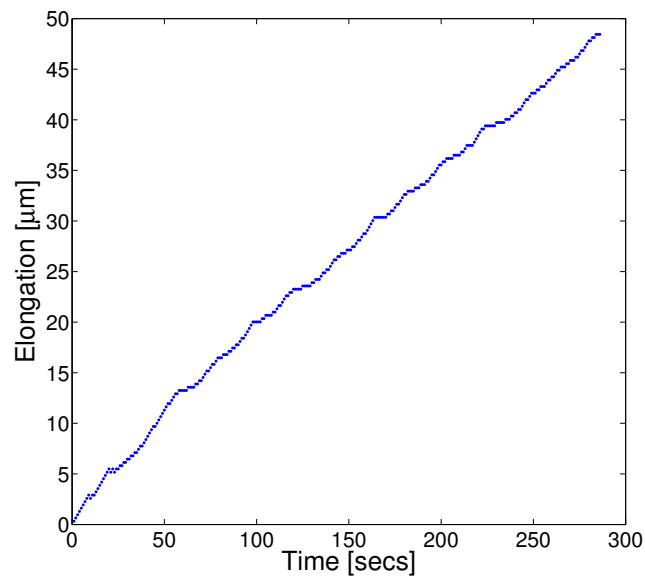


Fig C. Oscillatory tip growth of a lily pollen tube in the chip.

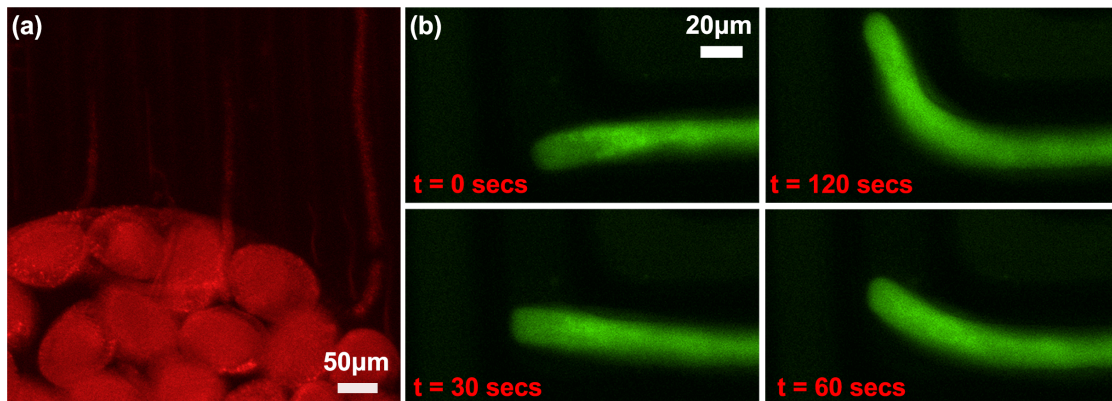


Fig D. Passive co-incubation staining of lily grains and tubes (a) Cell wall staining with propidium iodide and (b) Calcium Green<sup>TM</sup>-1 AM stained tube navigates a 90 degree bend in the microchannel.

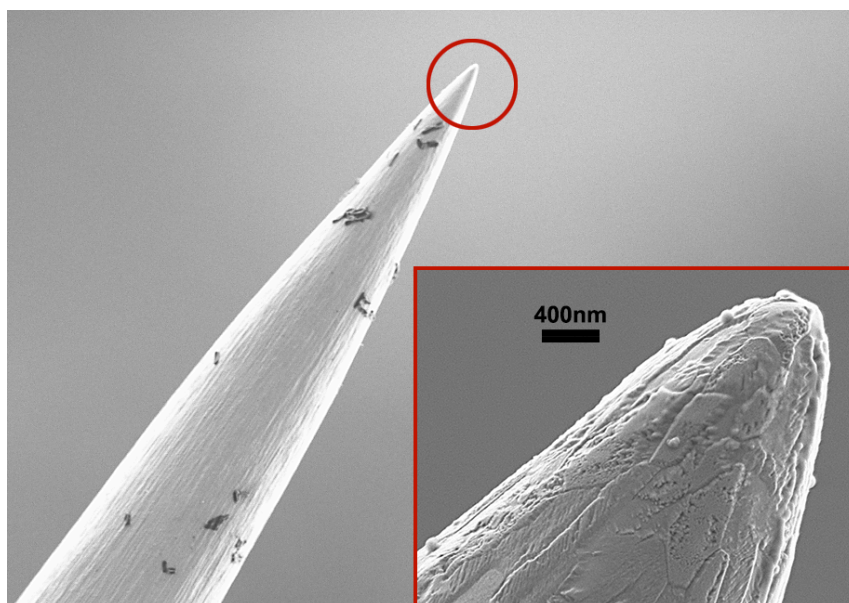


Fig E. SEM of CFM micro-indentation tip (Tungsten). The nominal tip diameter is 0.8 µm.

## Finite Element Method (FEM)-based Modeling

### Model Implementation

The mechanical modeling of the micro-indentation is implemented in COMSOL Multiphysics® Structural Mechanics module. In the three-dimensional FEM simulation environment, the pollen tube is geometrically modeled as a long cylindrical shell capped with a hemispherical dome and uniformly pressurized from within. A linear orthotropic material model is used for the cell wall, with the formulation as detailed previously [1,2]. Furthermore, the cell wall is assumed to be uniform in thickness and fully compressible, with the same radial and longitudinal elastic moduli. The shear modulus equals half of the longitudinal elastic modulus and the turgor pressure is homogenous across the whole volume. A mean circumferential stretch ratio  $\lambda_c = 10.2\%$  is obtained by pollen tube plasmolysis ( $n=16$ ), i.e., by replacing the growth medium with 15 % mannitol solution. The longitudinal stretch ratio  $\lambda_l$  is assumed to be half the circumferential stretch ratio [1]. The simulation is solved in a two-step process, where the non-turgid tube is pressurized with a given turgor pressure and in the second step the indenter is brought in contact with the tube and the indentation progresses iteratively.

We performed a parametric FEM study to account for the variability in turgor pressure, cell wall thickness, the overall dimensions of the pollen tube, and the elastic moduli on the experimentally measured spread in loading stiffness of the pollen tube. The indentation problem is solved for a multi-parameter range of cell wall thickness (100-700 nm), tube diameter ( $17.3 \pm 2.3 \mu\text{m}$ ) and turgor pressure (0.21, 0.30, and 0.4 MPa) reported for lily pollen tubes. We use a logarithmic strain model combined with the thin-walled pressurized cylinder approximation [3] to estimate the range of circumferential and longitudinal elastic moduli ( $E_c$  and  $E_l$ ) and the initial unpressurized pollen tube diameter for our simulations,



$$E_c = \frac{Pr}{t \log(\lambda_c)}; \quad E_l = \frac{Pr}{2t \log(\lambda_l)}$$

where  $P$  is the turgor pressure,  $r$  is the radius of tube, and  $t$  is the cell wall thickness. The linear elastic moduli thus become dependent variables and have been summarized in Table S3 for the range of cell wall thickness and turgor pressure used in combination with the measured range of tube diameters. The indentation point is always 60  $\mu\text{m}$  away from the apex of the tube.

### Choice of Input Parameters

Even though the ultrastructure and physiology of lily pollen tubes have been studied since the 1960s, there is a broad range in the measured values of cell wall thickness and turgor pressure, which are key parameters needed to estimate the elastic moduli. Cell wall thickness has a spatiotemporal modulation across the tube. It is thicker at the apex than in the shank, signifying the conversion of methyl-esterified pectins into  $\text{Ca}^{2+}$ -mediated cross-linked structures further down the length [4]. In addition, the apical cell wall in lily has been shown to modulate in thickness from 500 nm to 700 nm [5], with a period of 26 seconds corresponding to the growth oscillation cycle. From transmission electron microscopy (TEM) images, the reported thickness has a range from 110 nm to 400 nm [6], while an upper bound of 700 nm was previously reported using propidium iodide to stain the cell wall [1]. A measurement of the turgor pressure of lily pollen has been reported only twice. A value of  $0.209 \pm 0.064$  MPa ( $n=106$ ) was reported for growing lily tubes using micro-pipette injection and a value of 0.79 MPa ( $n=49$ ) by incipient plasmolysis [7], while an internal pressure of  $0.317 \pm 0.07$  MPa ( $n=17$ ) was reported in lily pollen grains by Pertl et al. [8], who also used a micro-injection technique.

Turgor pressure (MPa)	Cell wall thickness (nm)							Tube diameter ( $\mu\text{m}$ )
	100	200	300	400	500	600	700	

	Elastic moduli (MPa)							
<b>0.21</b>	161.41	80.70	53.80	40.35	32.28	26.90	23.06	<b>15</b>
	165.25	82.63	55.08	41.31	33.05	27.54	23.61	
<b>0.21</b>	185.08	92.54	61.69	46.27	37.02	30.85	26.44	<b>17.3</b>
	189.49	94.74	63.16	47.37	37.90	31.58	27.07	
<b>0.21</b>	210.90	105.45	70.30	52.73	42.18	35.15	30.13	<b>19.6</b>
	215.93	107.96	71.98	53.98	43.19	35.98	30.85	
<b>0.30</b>	230.58	115.29	76.86	57.64	46.12	38.43	32.94	<b>15</b>
	236.07	118.04	78.69	59.02	47.21	39.35	33.72	
<b>0.30</b>	264.39	132.19	88.13	66.10	52.88	44.07	37.33	<b>17.3</b>
	270.69	135.35	90.23	67.67	54.14	45.12	38.67	
<b>0.30</b>	301.29	150.35	100.43	75.32	60.26	50.22	43.04	<b>19.6</b>
	308.47	154.23	102.82	77.12	61.69	51.41	44.07	
<b>0.40</b>	307.44	153.72	102.48	76.86	61.49	51.24	43.92	<b>15</b>
	314.76	157.38	104.92	78.69	62.95	52.46	44.97	
<b>0.40</b>	352.53	176.26	117.5	88.13	70.50	58.76	50.36	<b>17.3</b>
	360.93	180.46	120.31	90.23	72.19	60.15	51.56	
<b>0.40</b>	401.72	200.86	133.91	100.43	80.34	66.95	57.39	<b>19.6</b>
	411.29	205.64	137.09	102.82	82.26	68.55	58.76	

Table A. The orthotropic elastic moduli ( $E_{\text{circumferential}}$ ,  $E_{\text{longitudinal}} = E_{\text{radial}}$ ) for varying cell wall thickness, turgor pressure and pollen tube diameters calculated from the logarithmic strain model.

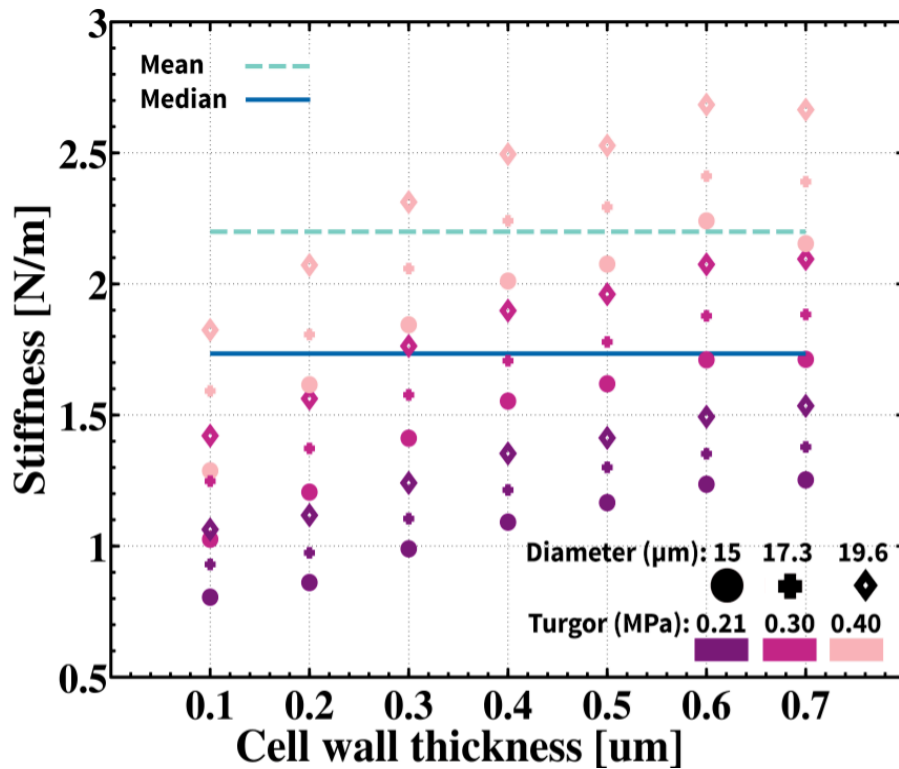


Fig F. Variation of the apparent stiffness of the cell wall of *Lilium longiflorum* pollen tube with varying cell wall thickness, turgor pressure, tube diameter as calculated by FEM analysis. The corresponding orthotropic elastic moduli can be found in Table S3. The experimentally measured mean and median of the loading force-indentation curves are marked on the graph. We note that several different combinations of the input parameters yield similar values of apparent stiffness.

## References:

1. Vogler H, Draeger C, Weber A, Felekis D, Eichenberger C, Routier-Kierzkowska AL, et al. The pollen tube: A soft shell with a hard core. *Plant J.* 2013;73: 617–627. doi:10.1111/tpj.12061
2. Weber A, Braybrook S, Huflejt M, Mosca G, Routier-Kierzkowska A-L, Smith RS. Measuring the mechanical properties of plant cells by combining micro-indentation with osmotic treatments. *J Exp Bot.* 2015;66: 3229–3241. doi:10.1093/jxb/erv135
3. Hearn EJ. *Mechanics of Materials, Vol 1.* Elsevier. Elsevier; 1997.
4. Wilsen KL, Hepler PK. Sperm Delivery in Flowering Plants: The Control of Pollen Tube Growth. *Bioscience.* 2007;57: 835. doi:10.1641/B571006
5. McKenna ST, Kunkel JG, Bosch M, Rounds CM, Vidali L, Winship LJ, et al. Exocytosis precedes and predicts the increase in growth in oscillating pollen tubes. *Plant Cell.* 2009;21: 3026–3040. doi:10.1105/tpc.109.069260
6. Anderson JR, Barnes WS, Bedinger P. 2,6-Dichlorobenzonitrile, a cellulose biosynthesis inhibitor, affects morphology and structural integrity of petunia and lily pollen tubes. *J Plant Physiol.* 2002;159: 61–67. doi:10.1078/0176-1617-00651
7. Benkert R, Obermeyer G, Bentrup F-W. The turgor pressure of growing lily pollen tubes. *Protoplasma.* 1997;198: 1–8. doi:10.1007/BF01282125
8. Pertl H, Pöckl M, Blaschke C, Obermeyer G. Osmoregulation in *Lilium* pollen grains occurs via modulation of the plasma membrane H<sup>+</sup> ATPase activity by 14-3-3 proteins. *Plant Physiol.* 2010;154: 1921–1928. doi:10.1104/pp.110.165696